Exploring the Mechanism, Advancements, and Application of Thermogalvanic Effect in Hydrogels

Xiaoyu Yang[1], Peng Wang[1], Xiaolong Wu[1], Yongli Liao[2], Senyun Liu[3], Wei Duan[1], and Ying Yue[1]

[1]North China Electric Power University - Baoding Campus
[2]China Southern Power Grid South Electric Power Research Institute
[3]China Aerodynamics Research and Development Center Key Laboratory of Icing and Anti/De-icing of Aircraft

July 3, 2023

Abstract

The issue of energy consumption has garnered significant interest due to its excessive usage. Recently, thermoelectric devices have been getting increased attention, as they can harness waste heat from various sources, such as solar radiation, human body, and industrial processes. Traditionally, the recovery of low-grade heat has been a challenge, resulting in unsustainable energy use and significant losses. While considerable advances have been made in thermoelectric materials in recent decades, the majority of these devices still primarily employ semiconductors. Nevertheless, the emergence of quasi-solid-state thermoelectric materials represents a novel devel-opment with profound promise for the environment and society. These materials offer several advantages, such as improved energy conversion capacities, cost-effectiveness, versatility, and scalability, to support increased usage. Additionally, this review explores the application of thermoelectric materials in self-powered sensors, integrated modules, and heat harvesting management. Lastly, the po-tential of high-performance thermocouples based on thermogalvanic effects is assessed, along with the challenges that must be over-come to realize this goal.

Cite this paper:*Chin. J. Chem.* **2023** , *41* , XXX—XXX. **DOI: 10.1002/cjoc.202300XXX**

Exploring the Mechanism, Advancements, and Application of Thermogalvanic Effect in Hydrogels

Xiaoyu Yang,[a,b] Peng Wang,*[,a,b] Xiaolong Wu,[a,b] Yongli Liao,[c]Senyun Liu,[d] Wei Duan,[a,b] and Ying Yue,[a,b]

[a] School of Energy, Power and Mechanical Engineering, North China Electric Power University, Baoding 071000, China[b] Hebei Key Laboratory of Electric Machinery Health Maintenance & Failure Prevention, North China Electric Power University, Baoding 071003, China[c] Electric Power Research Institute, China South Power Grid, Guangzhou 510000, China[d] Key Laboratory of Icing and Anti/De-icing, China Aerodynamics Research and Development Center, Mianyang, Sichuan 621000, China

Keywords

Hydrogel | Thermogalvanic Effect | Thermocell | Seebeck coefficient | Redox couple

Comprehensive Summary

The issue of energy consumption has garnered significant interest due to its excessive usage. Recently, thermoelectric device

After acceptance, please insert a group photo of the authors taken recently.	Xiaoyu Yang obtained his master's degree in S Prof. Dr. Peng Wang earned his bachelor's an Xiaolong Wu obtained his bachelor's degree in Yongli Liao is currently a senior researcher an Senyun Liu is currently working in the Key L Assoc. Prof. Dr. Wei Duan obtained her bach Assoc. Prof. Dr. Ying Yue obtained her bach
Left to Right: Author 1, Author 2, Author 3, ···	

Contents

1. Introduction

With the exponential increase in energy demand, there has been an excessive reliance on fossil fuels such as natural gas, oil, and coal, resulting in severe pollution, widespread environmental damage, and further aggravation of the global energy crisis.[1-6] Therefore, the pursuit of energy recycling has gained significant attention. Heat energy, which is derived from the burning of fossil fuels or solar radiation, serves as a widely utilized energy source. While heat can be partially recycled, the challenge lies in effectively reusing and capturing low-order heat generated by human activities, solar radiation, and electronic devices.[7–11]

Solid-state thermoelectric devices based on semiconductors have been widely researched and applied for the recycling of low-grade thermal energy. Nonetheless, it is important to acknowledge that the output performance of these semiconductor devices is temperature-dependent. Excessively high temperatures pose a risk of fracture in the p-n junction, resulting in considerable deterioration in performance. Conversely, extremely low temperatures reduce the thermoelectric properties of solid materials, resulting in remarkably low Seebeck coefficients ranging from 100 to 200 $\mu V\ K^{-1}$.[12,13] Currently, Bi_2Te_3 stands as the sole commercially utilized

solid-state material in this domain. [14]Temperature fluctuations threaten the performance stability, safety, and lifespan of electronics. Thus, maximizing the efficiency of thermoelectricity and exploring new avenues for its development have become prominent areas of research. In this context, hydrogels have emerged as a promising electrolyte medium. Current studies indicate that hydrogels exhibit two distinct working modes for the thermoelectric effect: thermogalvanic effect and thermal diffusion effect. Table 1 provides a simple comparison of the two modes. Thermogalvanic effect is a cost-effective option that offers flexible structural designs. Recent studies suggest that hydrogels utilizing the thermoelectric current effect can achieve Seebeck coefficients exceeding 1 mV K^{-1}.[15–22] Moreover, certain experimental samples can be coupled and integrated to achieve higher output voltages. This review primarily focuses on the discussion of hydrogels using redox reactions as a basis for thermoelectric devices. It aims to provide a comprehensive understanding of the fundamental principles, gel structures, and practical applications of such systems.

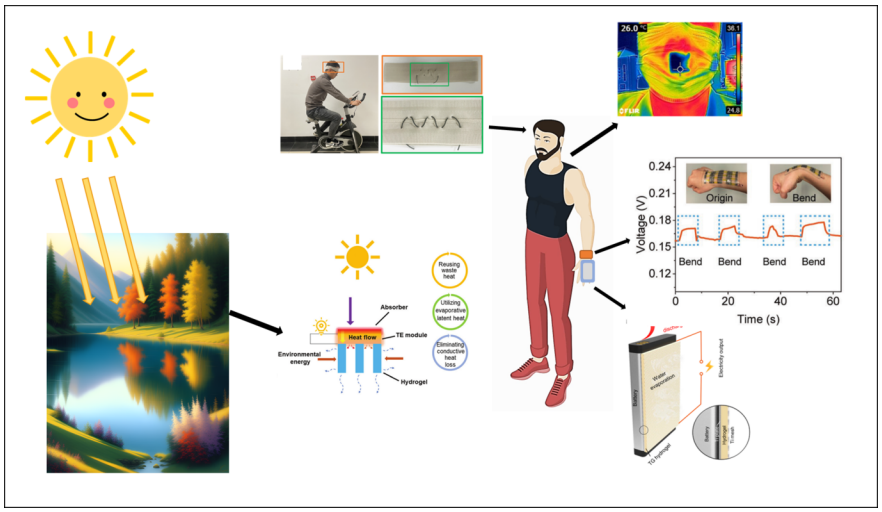

Figure 1 Applications of redox thermal cells rely on thermogalvanic effect. Application of integrated module[75](Reproduced from ref. 75 with permission from John Wiley and Sons, copyright 2022), respiratory monitoring[19](reprinted with permission from ref. 19. Copyright 2022 American Chemical Society), health management[89](reprinted with permission from ref. 89. Copyright 2022 American Chemical Society), heat collection management[91](reproduced with permission from ref. 91. Copyright 2022, Royal Society of Chemistry), battery heat recovery device[32](reprinted with permission from ref. 32. Copyright 2020 American Chemical Society) etc.

Table 1 Comparison of different types of thermalcells

Reaction principle	Reactant	Characteristics
Thermogalvanic effect	Redox couples	1)The Seebeck coefficient is smaller 2) It mainly works in the operation mode of thermal battery
Thermal diffusion effect	Polymer ion thermoelectric material	1) The Seebeck coefficient is larger 2) The source of electricity is intermittent heat 3) It mainly works in the operation mode of thermal capacitance

2. Development and application of the thermogalvanic effect in the field of electrochemistry

2.1. Working Principle of Redox Reaction Thermocouple

This review delves into the exploration of thermocouples and their utilization in generating thermal potential through the exploitation of the thermogalvanic effect. The thermogalvanic effect finds typical applications in thermoelectric cells, wherein redox couples such as$[Fe(CN)_6^{4-}/Fe(CN)_6^{3-}]$, $[Fe^{2+}/Fe^{3+}]$and $[I^-/I_3^-]$ are employed to convert heat energy into electricity, as illustrated in Figure 2. Usually, these redox couples, along with electrolytes, can reach a certain degree of the Seebeck coefficient. The Seebeck coefficient of ionic thermoelectric materials based on the thermogalvanic effect is determined by Eq. (1) as follows:[23]

$S = \frac{V}{T} = \frac{S}{nF}$ (1)

where V, S, n, and F represent the open circuit operating voltage of the ionic thermoelectric material, the partial molar entropy difference of the redox couple, the number of electrons transferred during the redox reaction, and the Faraday constant, respectively. When considering the Seebeck coefficient, the energy conversion efficiency of thermoelectric materials is often determined using the dimensionless quality factor, defined by Eq. (2) as follows:[24]

$ZT = \frac{S^2\sigma T}{}$

englishk=$\Sigma^2\sigma$T

ενγλισηη$(\varkappa_e + k_l)$(2)

ωηερε S ρεπρεσεντς τηε Σεεβεςκ ςοεφφιςιεντ, σδενοτες τηε ςονδυςτιιτψ οφ τηε ματεριαλ, T ρεπρεσεντς τηε αβσολυτε τεμπερατυρε, ανδ k ρεπρεσεντς τηε τηερμαλ ςονδυςτιιτψ. Σπεςιφιςαλλψ, k_e δενοτες τηε ελεςτρον τηερμαλ ςονδυςτιιτψ ωηιλεk_l ις τηε λαττιςε τηερμαλ ςονδυςτιιτψ. Ινδεεδ, αςηιεινγ α ηιγηZT αλυε ςορρεσπονδς το α ηιγηερ ενεργψ ςονερσιον εφφιςιενςψ ιν τηερμοελεςτρις ματεριαλς. Τηε διφφερενςε ιν ρεδοξ στατες σιγνιφιςαντλψ ινφλυενςες τηε εντροπψ οφ ιον παρτιαλ μολες βετωεεν διφφερεντ αλενςε στατες ανδ δετερμινες ιτς S. Αδδιτιοναλλψ,$S^2\sigma$ ςαν βε ιντερπρετεδ ας τηε τηερμοελεςτρις ποωερ φαςτορ. Το ατταιν ηιγη ZT αλυες, ιτ ις ςρυςιαλ το ηαε α ηιγηερ$S^2\sigma$ ωηιλε μινιμιζινγ τηεk. Τηις ινσιγητ ηιγηλιγητς α διρεςτιον φορ ιμπροινγ τηε τηερμογαλανις εφφεςτ οφ ιονις τηερμοελεςτρις ματεριαλς.

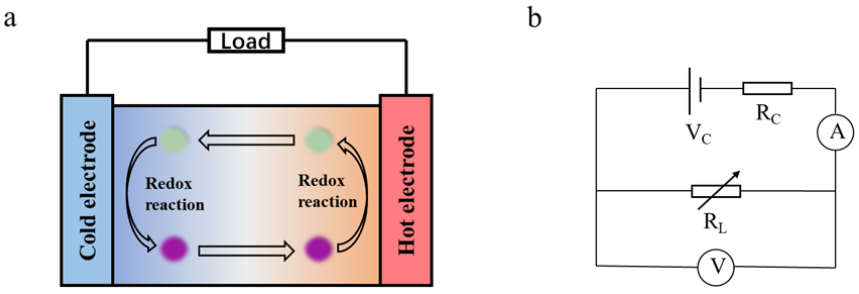

Figure 2 (a) Composition and working principle of thermocouple based on redox reaction. (b) Thermocouple working equivalent circuit. Reproduced with permission from ref. 99. Copyright 2021, American Chemical Society

Thermoelectric devices can be categorized into p-type and n-type based on the value of the thermal potential, as illustrated in Figure 3. The p-type devices typically exhibit a negative thermal potential, inducing an oxidation reaction at the thermal end. Consequently, electrons flow from this end to the cold end through an external circuit, generating a reduction reaction at the cold end. In contrast, n-type thermoelectric devices operate in the opposite manner, with positive thermal potential.[25]Typical examples of p-type redox couples include $[Fe(CN)_6^{4-}/Fe(CN)_6^{3-}]$, $[FeBr_4^{2-}/FeBr_4^-]$, and $[FeCl_4^{2-}/FeCl_4^-]$. On the other hand, common n-type redox couples consist of $[Co(byp)_3^{3+}/Co(byp)_3^{2+}]$, $[Fe^{3+}/Fe^{2+}]$, $[Cu^{2+}/Cu^+]$, $[Zn^{2+}/Zn^+]$, and $[I^-/I_3^-]$.

The effects and characteristics of different redox couples can vary significantly. Table 2 provide a simple comparison of commonly used redox couples with their respective properties.

Table 2 Comparison of different redox couples properties

Redox couples	Absolute charges and structure	S (mV K^{-1})	S (mV K^{-1})	Ref.
$Fe(CN)_6^{4-}/Fe(CN)_6^{3-}$	High absolute charges and complex structures	4.28	92	92
$Fe(\mathrm{Clo}_4)_2/Fe(\mathrm{Clo}_4)_3$	High absolute charges and complex structures	1.76	95	95
SO_3^{2-}/SO_4^{2-}	Low absolute charges and simple structures	1.63	93	93
Fe^{3+}/Fe^{2+}	Low absolute charges and simple structures	-1.63	15	15
I^-/I_3^-	Low absolute charges and simple structures	0.51	96	96

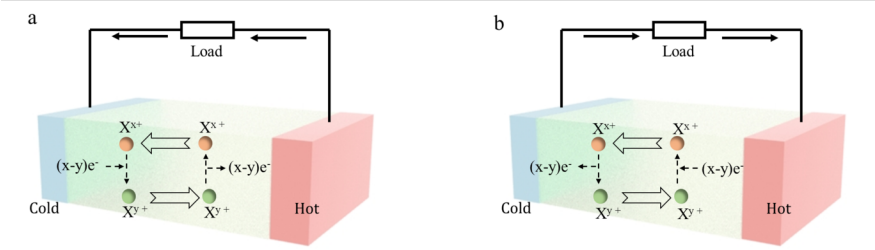

Figure 3 (a) is a p-type thermocouple and (b) is an n-type thermocouple. $M^{m+}$and M^{n+} stands for redox couples.

2.2. Factors affecting thermocouples based on thermogalvanic effect

2.2.1. Impacts of hydrogel composition

Traditional semiconductor thermoelectric materials demonstrate a favorable S at high temperatures. However, when being utilized in absorbing and converting low-degree heat energy, their coefficients plummet to below 200 μV K^{-1}, exacerbating the unfavorable issue of material flexibility. Quasi-solid electrolytes, such as hydrogels, address these issues by presents a safer, efficient, environmentally friendly, and flexible alternative.[26]

Ionic gels possess a broad operating temperature range, enhanced ionic conductivity, and higher S , making them ideal for energy conversion and utilization. At the same time, gels offer diverse applications, further highlighting their versatility. A notable example is the study conducted by Wang et al. in 2021, where they utilized gels and functional carbon nanomaterials to prepare a flexible supercapacitor.[27] The study discusses the ionotropic gelation properties when introduced into various matrices, with particular attention to its impacts.

In recent years, there has been a considerable focus on hydrogel electrolytes as flexible quasi-solid polymers. These hydrogels are developed through the chemical or physical crosslinking of hydrophilic natural or synthetic polymers. Polysaccharides and polypeptides are frequently used as natural hydrophilic polymers in the preparation of hydrogels. Meanwhile, synthetic hydrophilic polymers include but are not limited to, acrylic acids, alcohols, and their derivatives.[28] Among them, polyacrylamide (PAAm) and polyvinyl alcohol (PVA) are two of the most commonly employed hydrophilic polymer materials in research studies.

Acrylamide (AM) is an organic compound that readily polymerizes via ultraviolet irradiation or at high temperatures due to the presence of a carbon-carbon double bond and amide group. PAAm hydrogels exhibit remarkable resilience and excellent elasticity, as well as mechanical and chemical stability. [29–31] The chemical

properties of these hydrogels can be adjusted by controlling the gel pore size via varying the concentrations of monomers and cross-linkers, thereby tailoring their usage conditions accordingly. In this regard, Hu et al.[32] prepared a smart thermocouple hydrogel film achieving efficient evaporative cooling and waste-heat recovery (Figure 4). The study investigated the recycling of$[Fe(CN)_6^{4-}/Fe(CN)_6^{3-}]$ redox couple to drive redox thermoelectricity, harnessing K^+, Li^+,Br^-,and$[Fe(CN)_6^{4-}/Fe(CN)_6^{3-}]$plasma confined in either water or polymer to enhance thermoelectric conversion. Moreover, the moisture content of hydrogels was regulated through the controlled equilibrium of Li^+ and Br^- ions. Meanwhile, any excess heat generated was dissipated by the evaporation of free water molecules present in the hydrogel. High mechanical strength and an impressive tensile strain of 0.24 MPa allow hydrogels to elongate 2–3 times beyond their original length. Further, Wu et al.[18]introduced a double network hydrogel, incorporating AM and AMPS with remarkable thermal and electrical capabilities. As depicted in Figure 4c, the hydrogel demonstrated exceptional tensile strength, enabling it to lift a 1.5 kg fruit without being ruptured. Additionally, this hydrogel displayed around 220% elongation under stress levels of nearly 1200 kPa (Figure 4d). In order to obtain a hydrogel with a combination of high tensile strength, superior elongation, and excellent thermal and electrical efficiency, Chen et al.[22]employed a double-network structure composed of PAAm/Alg. This as-obtained hydrogel displayed outstanding tensile strength (up to 700%), as shown in Figures 4e and 4f. Further, the elastic modulus, fracture stress, and elongation of the hydrogel were also recorded. Collectively, these findings suggest the promising potential of AM-based hydrogels in single/double network systems.

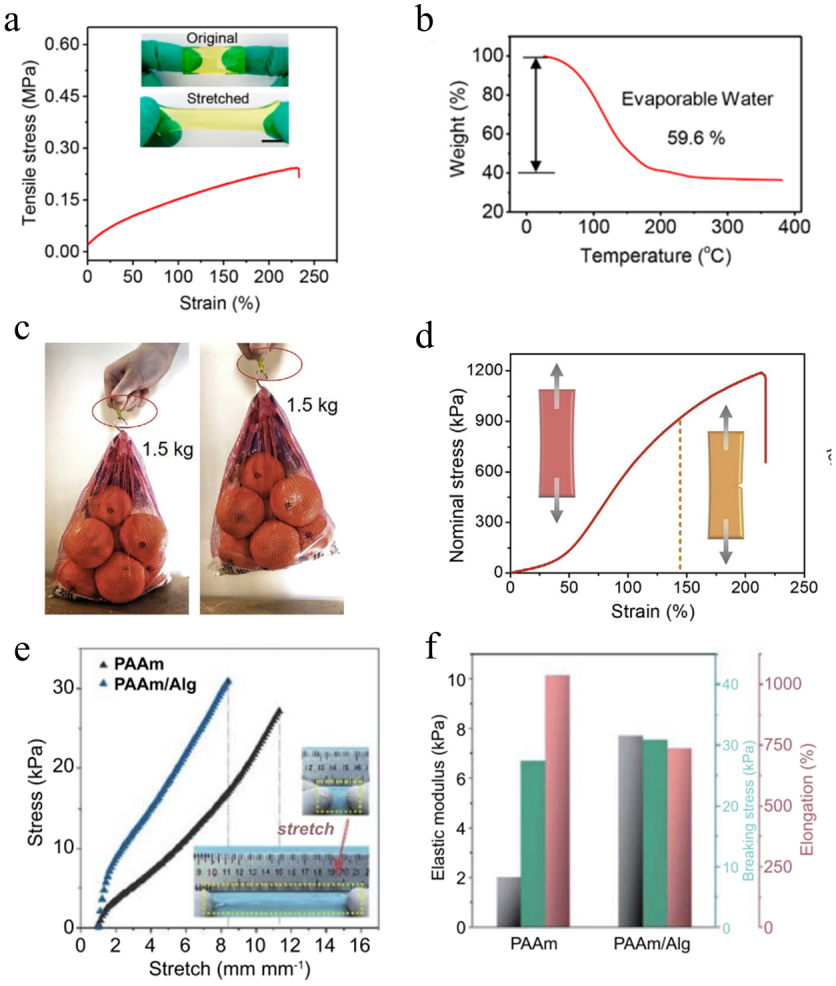

Figure 4 (a) Stress-strain curve of the hydrogel. The tests were carried out with a stretching rate of 20 mm min-1. Insets show pictures of the TG hydrogel in its original and stretched state. The scale bar is 1 cm. (b) Thermogravimetric characterization of thermogalvanic hydrogel. Reprinted with permission from Pu et al. Copyright 2020, American Chemical Society. (c) The double-network thermocell with a thickness of 3 mm and a width of 5 mm lifts a bag of oranges with a weight of 1.5 kg. The red circle indicates the location of the thermocell. (d) The nominal stress-strain curve of the double-network thermocell (un-notched). The yellow dashed line indicates the strain-at-break of a notched sample. Reproduced with permission from Lei et al. Copyright 2021, Elsevier. (e) Stress-strain curves of the PAAm and PAAm/Alg hydrogels. Inset shows the stretching process of the PAAm/Alg hydrogel, which can be easily stretched over 700%. (f) The elastic modulus, breaking stress, and elongation data of the PAAm and PAAm/Alg hydrogels.[22]Copyright 2022, Springer Nature.

Meanwhile, the thermoelectric properties of these hydrogels are the biggest concern. Hu's TG hydrogel exhibits favorable physical and electrochemical properties.Figure 5a depicts the thermoelectric properties of the hydrogel, including the$S$ is 1.2 mV K^{-1}, theeffective conductivity of approximately 100 mS/cm, and the thermal conductivity ranging from 0.30 to 0.39 W $(mK)^{-1}$, and the power generation factor of 6.5-12 $\mu W(m\ K^2)^{-1}$. Chen et al. observed a remarkably significant Svalue of up to 1.43 mV $K^{-1}$for the PAMM/ALg hydrogel, while simultaneously retaining high stretchability. Previously, Wu et al. achieved a remarkably high$S$value of 1.5 mV K^{-1} for their double-network thermocell, influenced by the concentration of NaCl. Despite the satisfactory thermoelectric performance of hydrogels, there is ample opportunity for improvement.

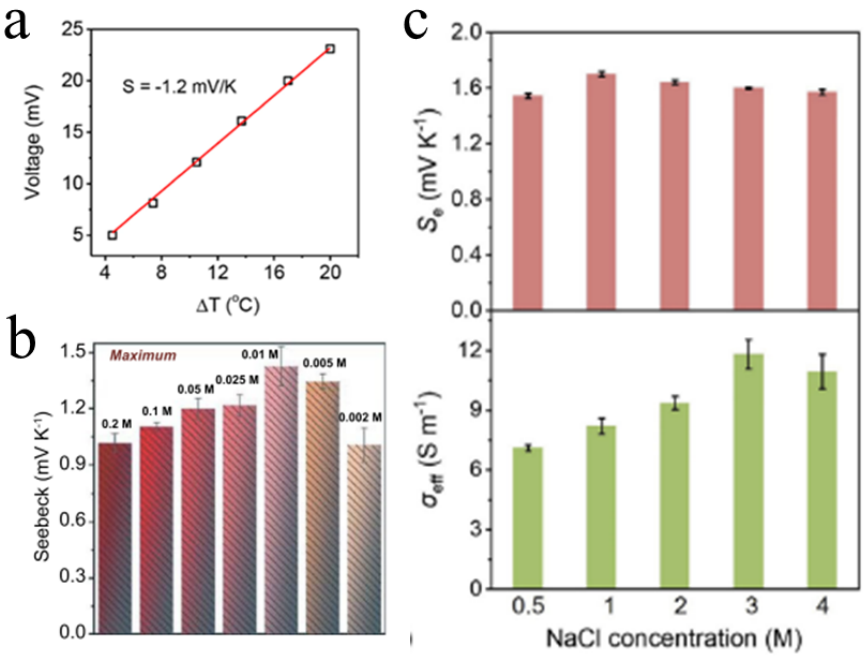

Figure 5 (a) Dependence of the output voltage on applied temperature differences. Reprinted with permission from ref. 32. Copyright 2020 American Chemical Society. (b) Comparison of the maximum$S$ of different PAAm/Fe-Alg hydrogels (the Se at 0.25 h for the 0.2, 0.1, 0.05, 0.025, 0.01, and 0.005 M samples, and the Se at 6 h for the 0.002 M sample).[22]Copyright 2022, Springer Nature.(c) $S$and σ of the thermocells with different NaCl concentrations. The $[Fe(CN)_6^{4-}/Fe(CN)_6^{3-}]$ concentration is fixed at 0.4 M. Error bar represents standard deviation. Reproduced with permission from Lei et al.. Copyright 2021, Elsevier.

Furthermore, PVA possesses excellent characteristics that make it a potential matrix for the development

of hydrogel electrolytes. It is cost-effective, easily processed, and can be formed into films with outstanding bending performance.[33–40] In the 1980s, Petty-Weix et al.[41] made significant progress by developing a proton-conductive polymer electrolyte from PVA/H_3PO_4, which showed high ionic conductivity. PVA servesas an ideal matrix for quasi-solid thermocell sowing to its desirable characteristics such as biocompatibility, non-toxicity, non-corrosiveness, and excellent water solubility.[42–47] Along these lines, Wu et al. successfully developed a quasi-solid thermal cell that mimics the structure of layered fibrils and organized nanochannels found in natural muscles.[36] PVA was employed as a matrix in this system, facilitating the permeation of $[Fe(CN)_6^{4-}/Fe(CN)_6^{3-}]$ redox couple into the hydrogel via solvent exchange. Moreover, it was observed that mechanical training strengthens the hydrogen bonding within the PVA chain; however, it weakens the interaction between the PVA chain and water molecules. Consequently, this released additional water molecules, thereby promoting ion conduction within the polymer networks. As demonstrated in Figures 6a and 6b, the quasi-solid heat cell showcased a tensile strength of 470%, along with toughness and fatigue thresholds of 17900 J m^{-2} and 2500 J m^{-2}, respectively, surpassing those of natural muscles. In another attempt, Zhang et al.[93]introduced a novel redox couple as PVA-$SO_{4/3}{}^{2-}$ gel, displaying remarkable tensile properties. The gel demonstrated its strength by easily lifting a weight of 1 kg, as depicted in Figure 6c. Notably, the gel exhibited an impressive tensile strength of up to 833 kPa, with a tensile strain of approximately 220%. Furthermore, the combination of dimethyl sulfoxide (DMSO) and PVA has recently garnered attention. In this direction, Zhang et al.[94] capitalized on this combination to develop a thermogalvanic gel. As shown in Figure 6e, the presence of DMSO greatly enhanced the tensile strength of the gel at the expense of reduced tensile strain. However, the introduction of ethylene glycol (EG) helped in attaining the maximum Young's modulus of up to 0.217 MPa.

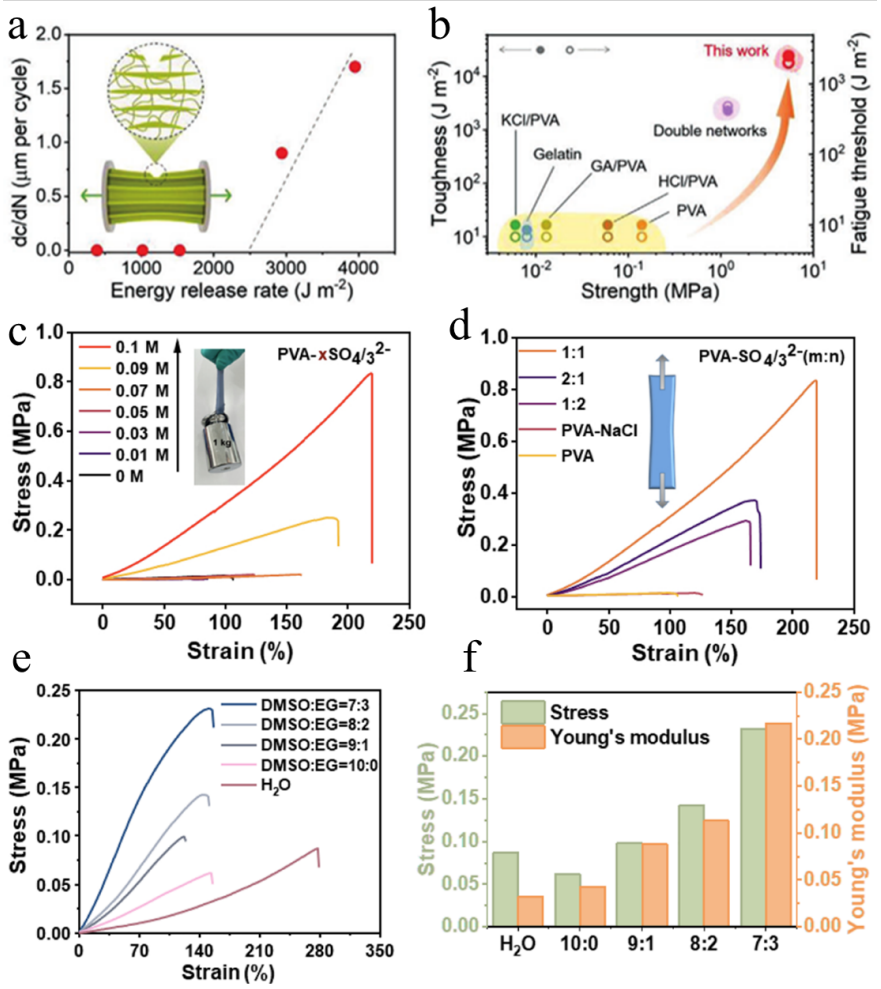

Figure 6 (a) Crack propagation per stretching cycle (dc/dN) of the thermocell under increasing energy release rate. (b) A comparison of the mechanical properties (toughness, fatigue threshold, and strength) between the thermocell and existing quasi-solid thermocells with mechanical records. The yellow, blue, and purple regions represent the quasi-solid thermocells based on physically crosslinked, chemically crosslinked, and double-networks, respectively. Reproduced with permission from Lei et al. Copyright 2022 Wiley-VCH.[36] (c) Mechanical properties of PVA-$SO_{4/3}{}^{2-}$ hydrogels. Stress-strain curves of hydrogels with different concentrations of the redox couple, the illustration shows a hot cell hydrogel with a thickness of 2 mm and a length of 5 cm lifting a weight of 1 kg. (d) Tensile stress-strain curves of the hydrogels with varying ratios of the redox couple. Reproduced with permission from Tian et al. Copyright 2023, Elsevier.[93] (e) Mechanical properties of the organogel. The tensile stress-strain curves of organogels with varying EG contents. (f) Stress and Young's modulus values of organogels with varying EG contents. Reprinted with permission from Fang et al. Copyright 2023, American Chemical Society.[94]

In addition, to facilitate the operation of thermal batteries at low temperatures, Chen et al.[48] considered the effects of solubility and used Fe(II/III) redox couples as thermocouples. They observed a significant reduction in the entropy elasticity of the polymer chain, along with limitations on the entropy difference of the redox ions. In order to break the strong hydrogen bond within the aqueous quasi-solid thermal cell, EG was introduced to lower the freezing point of the electrolyte solution to -40 °C. Additionally, Ma et al.[92] conducted comprehensive investigations on gels designed for extreme temperature conditions and suc-

cessfully developed a stretchable thermogalvanic hydrogel thermocell, exhibiting an unprecedented specific output power density through ion-induced effects. Surprisingly, the gel retained its functionality at a high temperature of 75 °C, highlighting its robustness. Moreover, to evaluate its performance at low temperatures, the cold end was set at -35 degC, and the gel continued to maintain its exceptional working state. This ground-breaking research signifies the immense potential of the developed gel for diverse applications, particularly in extreme temperature conditions. Recent work by Feng et al. has resulted in the development of cellulose-based thermogalvanic cells (TGC) with excellent mechanical properties.[97] To further enhance its capabilities, LiBr was added into the system, resulting in an expanded operating temperature range for the cell, which functioned between -50 degC and 50 degC, as demonstrated in Figures 7d and 7e. This innovative approach holds great potential and warrantsfurther exploration for its use in various applications. Overall, these studies provide valuable insights into the advancement of high-performance thermocell materials.

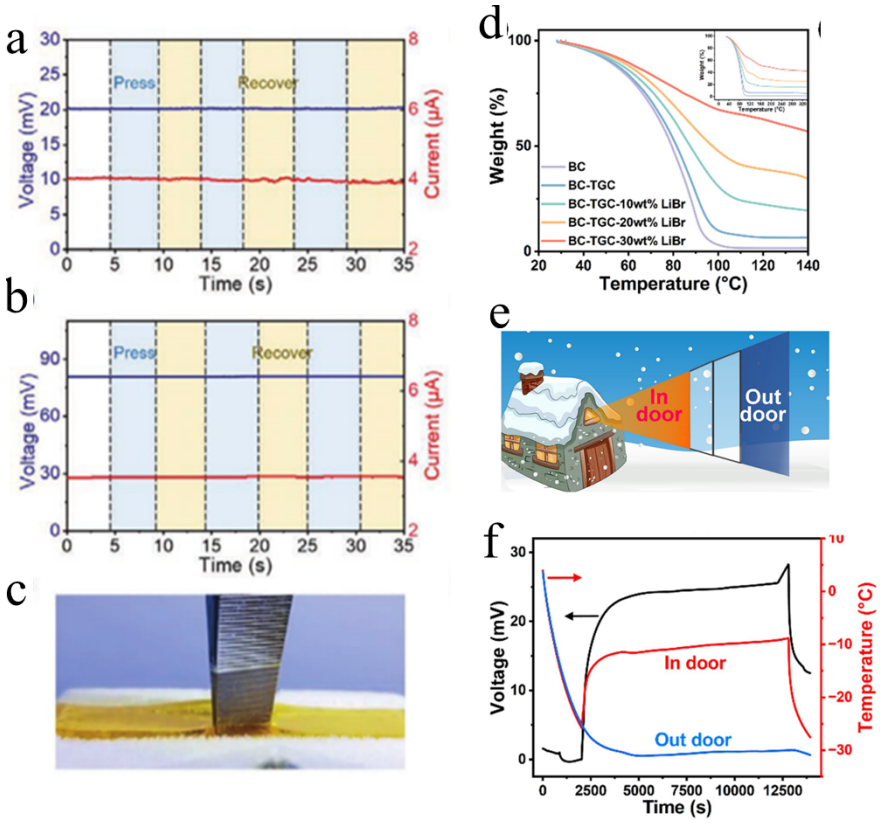

Figure 7 The output voltage and current of the organohydrogelthermocell during deformation: (a) The voltage-time (blue) and current-time (red)curves of the organohydrogelthermocell being repeatedly pressed when Tc = 20 °C and Th = 30 °C. (b) The voltage-time (blue) and current-time (red)curves of the organohydrogelthermocell being repeatedly pressed when Tc = -20 degC and Th = 20 degC. (c) A photograph of the organohydrogel thermocell being pressed on an ice surface of -20 degC. Reproduced with permission from Gao et al. Copyright 2021, Wiley-VCH.[48] (d) Thermogravimetric characterization of BC, BC-TGC, and BC-TGC with different LiBr weight fractions. (e) Schematic of TGC used as smart windows. (f) The corresponding voltage and temperature-time diagram of (e). Reproduced with permission from Yin et al. Copyright 2023, Elsevier.[97]

Gelatin, a polypeptide polymer, contains numerous polar groups such as -COOH, -NH_2, and -OH; thus, it exhibits strong polarization ability under the action of an electric field.[49–51] Using this property, Chen et al. developed a gelatin-based device that achieved a considerable thermoelectric conversion effect by combining

alkali metal salts with iron-based reduction couples.[52]This device demonstrated the ability to effectively harness energy from body heat and achieved a high thermoelectric energy of 17.0 mV K^{-1}. It was noticed that the ion transport in gelatin occurred by the thermal diffusion of KCl, NaCl, and KNO_3. Additionally, the thermoelectric effect was increased by the presence of $[Fe(CN)_6^{4-}/Fe(CN)_6^{3-}]$. This enhancement enables wearable devices, utilizing body heat energy as a heat source, to obtain a thermoelectric effect of 2 V and a maximum ΔT power of 12.8 J m^{-2}.

2.2.2. Impacts of structure design

The impact of different surface structures on hydrogels can lead to variations in heat absorption,[53] moisture retention,[54] wear resistance, etc. For mechanical or wearable devices, the overall shape of the hydrogel can be molded according to the specific needs of the device, facilitating effective heat dissipation. Furthermore, to achieve an optimal morphology, the microstructure of hydrogels should be intentionally designed based on actual requirements.[54–59]

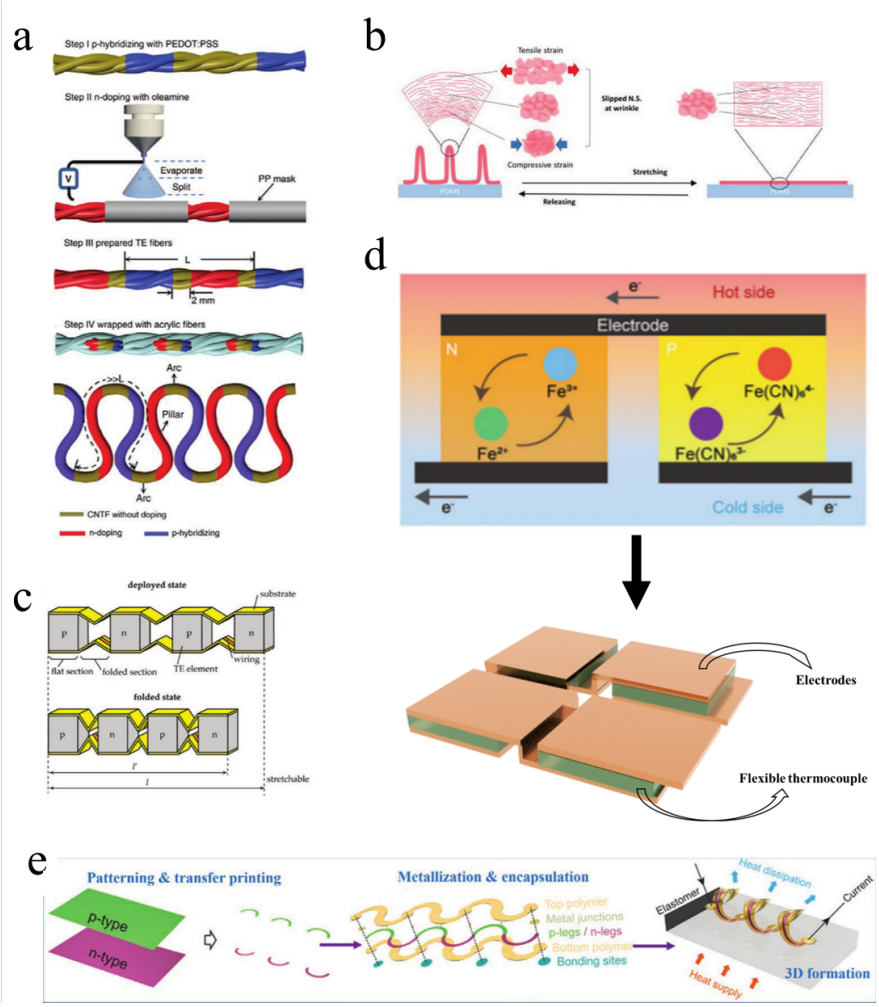

Figure 8 (a) Fabrication process illustration of the knitted fabric integrated TEG.[70] (b) Schematic illustration of the mechanism for thermoelectric material with wrinkle structure.[66] Reproduced from ref. 66 with permission from AIP Publishing, copyright 2019. (c) Schematic diagram and photographs of the stretchable TEG using origami-like folding deformation.[63] Copyright 2018, MDPI. (d) Illustration of the mechanism of connected p-n cell based on hydrogel electrolytes.[75] Reproduced from ref. 75 with permission from John

Wiley and Sons, copyright 2022. (e) Schematic illustration for fabrication of stretchable TEG with 3D helical architecture.[68] Copyright 2018, American Association for the Advancement of Science.

Surface structure engineering involves designing the surface microstructure of an ion polymer matrix, creating a gap between the electrode and the matrix.[60] The gap thus created enhances the compressibility of the hydrogel, leading to improved sensitivity and a broader range of response. Interestingly, external mechanical forces can alter the contact area between the ionic polymer matrix and the electrode.[61] At present, the surface structure of hydrogels can be classified into several types, including folding structure,[62,63] wrinkle structure,[64–66] spiral structure,[67,68] textile integration structure,[69,70] and island bridge structure with retractable electrodes,[71–75]as shown in Figure 8. Among them, the island bridge structure has gained widespread popularity due to its ability to preserve the mechanical properties of thermoelectric materials. It presents a simple construction process and scalability, making it suitable for the development of electronic skin applications. However, the performance of this structure relies heavily on electrode materials, and in current research, copper tablets are predominantly used as electrodes in the structure. The island bridge structures have been found to increase the flexibility of hydrogels in energy devices, although their operational lifespan can be somewhat affected. Moreover, the paper folding structure in hydrogels can enhance their tensile strain performance and is recognized as a powerful tool in the pursuit of obtaining complex 3D configurations and unprecedented performance through the graphic design of conventional materials. The folding structure is known for its stability, generally forming at the bonding interface of hydrogels through stretching or external influences. In contrast, the spiral structure directly improves the strain of thermoelectric hydrogels and reduces the influence of the environment on their conductivity. Similarly, the integration of thermoelectric generators (TEG) into textiles presents a favorable structure due to their malleability, lightweight, comfort, and air permeability, allowing for increased heat contact between thermoelectric materials and heat sources in a 3D interlocking mode.

2.2.3. Impacts of electrode materials

After discussing the influence of electrolytes as cells or capacitors, it becomes evident that electrodes play a key role in determining the performance of thermoelectric devices, considering their working principle. Wang et al. combined gel with meso/microporous graphene nanocomposites to prepare a flexible supercapacitor with excellent electrochemical performance.[76] Herein, we mainly focus on metal and carbon-based material electrodes, which are currently the most widely used electrode types in the field of energy storage and batteries.

Various metal-based electrodes, such as Ni,[77]Cu,[78,79] and W [80]electrodes, have been developed so far for thermal cells. As shown in Figure 9a,[81] the Ni-based thermal cells show similar performance to Pt foils, making them promising alternatives to Pt or nanostructured carbon electrodes under alkaline conditions. Additionally, Cu electrodes have also demonstrated advantages for thermal batteries. Duan et al. (Figure 9b)[82]reported a basic Cu electrode with a power density of 0.06 W m^{-2}, which was effectively improved to 0.75 W m^{-2} after modification to a 3D multi-structured Cu electrode. Moreover, the 2D Au/Cu electrode was modified to a 3D Au/Cu electrode configuration, resulting in a remarkable improvement in power density by 1072%. These outcomes imply that optimizing the electrode structure can effectively enhance the power density of the system.

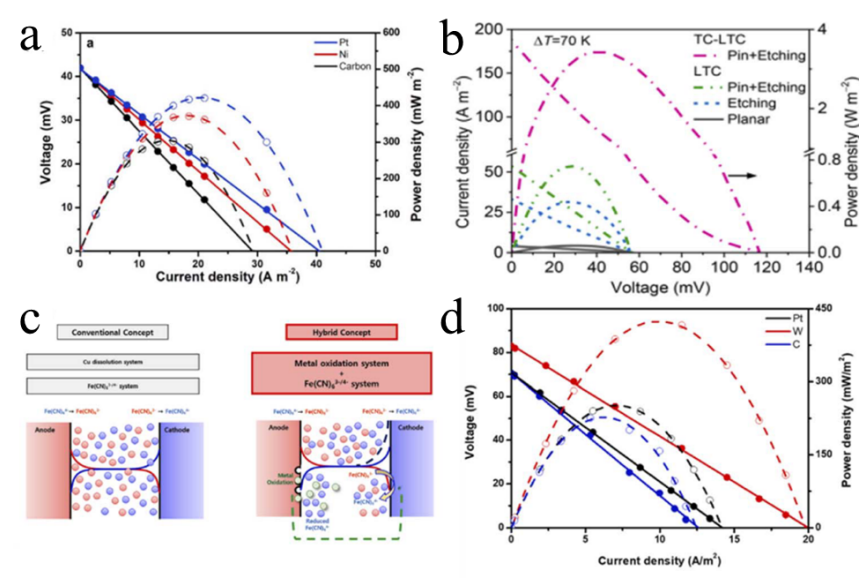

Figure 9 (a) Voltage (straight line) and power density (dashed line) versus current density of the Pt, Ni, and carbon electrodes.[81] Reproduced from ref. 81 with permission from Elsevier Ltd, copyright 2021. (b) Current-voltage and power-voltage curves for LTC and TC-LTC using different electrodes at a ΔT of 70 K. The best performance of the device was obtained using a 3D multi-structured Cu electrode.[82] Reproduced from ref. 82 with permission from Elsevier Ltd, copyright 2021. (c) Schematic diagrams of hybrid therermos-electrochemical cells (TECs). (d) Voltage (straight line) and power density (dashed line) versus current density of the Pt, W, and GC electrodes at ΔT of 50 K.[83]Reproduced from ref. 83 with permission from Elsevier Ltd, copyright 2021.

In the case of a W-based electrode, the S can be improved by two synergistic reactions, as depicted in Figure 9c: the redox reaction of the electrolyte and the oxidation reaction of the W electrode.[83] The resulting hybrid thermal cell using W electrodes achieved a S of 1.66 mV K^{-1}and a power density of 425 mW m^{-2}. Notably, this power density is 70% higher than that achieved by Pt or C electrodes, as shown in Figure 9d. This study presents a new thermal cell design employing metal-based electrodes, where both the electrodes and electrolytes undergo redox reactions. Generally, most metal-based electrodes possess varying valence states, and thus, this strategy provides another way to improve the performance of thermal batteries.

Furthermore, organic electrochemical devices are extensively used in the fields of bioelectronics, energy storage, electrocatalysis, and sensing. These devices operate based on a faradaic process, i.e., involving charger transfer through either oxidation reactions (electron loss) or reduction reactions (electron gain) facilitated by conductive polymers.

Berggren and Malliaras[84] demonstrated a simple metal electrode model that involves capacitive charge transport and storage of opposite charges in two electrode plates. On the other hand, they presented that a Faradaic process occurs with redox reactions on the bipolar plate, enabling charge transport and subsequently leading to a rectangular cyclic voltammetric curve that represented a transient charge current. Contrastingly, the voltammetric curves of the latter yield distinct redox peaks with the presence of a steady-state current. In addition, Horike et al. designed a flexible electrode using a polymer matrix derived from PEDOT: PSS. Their hydrogel samples were composed of Emim:Cl/PVA. While thermal diffusion is the predominant effect observed in this hydrogel, it still holds certain value to reference. The hydrogel, combined with this electrode, exhibited n-type conversion and showed a S of approximately 1 mV K^{-1}.[85]

Next, the carbon electrode is a carbon-based conductive material made by processing anthracite coal, petroleum coke, graphite, coal asphalt, etc., through molding, roasting, and machining. It is a new, energy-

saving, and environmentally friendly material that has gained increasing global usage since the 21st century. Carbon nanotubes (CNTs), discovered in the early 1990s,[86] are seamless, hollow nanoscale tubular structures made of single or multiple layers of graphite carbon, possessing unique physical and chemical properties. CNTs exhibit a range of impressive properties such as metal- or semiconductor-like conductivity, extraordinary mechanical strength, hydrogen storage capacity, broadband electromagnetic wave absorption, and significant adsorption capacity.[87] As a result of these exceptional properties, they hold important application value as energy storage materials, conductive materials, nanoelectronic components, and composite materials. Additionally, owing to their distinctive hollow structure, excellent conductivity, large specific surface area, and ion-permeable pores in electrolytes, coupled with their ability to intertwine and form nanoscale mesh structures, CNTs are often used as electrode materials in double-layer capacitors.

In a study conducted by Liu et al.,[88] a multi-walled CNT (MWCNT)-based ink was prepared with high viscosity and uniformity through ultrasonic treatment. It was demonstrated that chitin nanocrystals (ChNCs) interacted with MWCNT through non-covalent interactions like ?-? stacking and hydrophobic interactions. The ChNCs/MWCNT (CCNT) ink exhibited excellent stability, with no accumulation even after 3 months. By using CCNT ink, a paper-based TEG was produced utilizing the silk screen printing technique. Further, the CCNT dispersion underwent solvent evaporation, resulting in a self-supporting membrane with an electrical conductivity of up to 1150 S m^{-1}. The TEG was observed to have good biosecurity and flexibility, with the CCNT ink evenly attaching to both the surface and upper inner layers of the cellulose paper. Under a temperature difference of 12 K, the CCNT-based TEG showed efficient conversion of thermal energy into electrical energy, yielding a maximum output voltage of 0.375 mV, with a corresponding temperature difference of 0.7 K.

2.3. Application aspects and experimental scenarios of thermogalvanic hydrogels

2.3.1.Thermal induction self-supply equipments

In recent years, gels have generated significant interest in the fields of self-powering, status detection, and sensors.[98] Additionally, thermoelectric materials, based on thermoelectric principles, have been primarily employed as temperature sensors. However, there has been a growing focus on thermoelectric-based inductors due to their lower cost, simplified manufacturing processes, and ease of obtaining heat sources. They can monitor temperature, movement, and biophysical activities in wearable electronic devices, electronic skin, flexible robots, and other related scenarios.

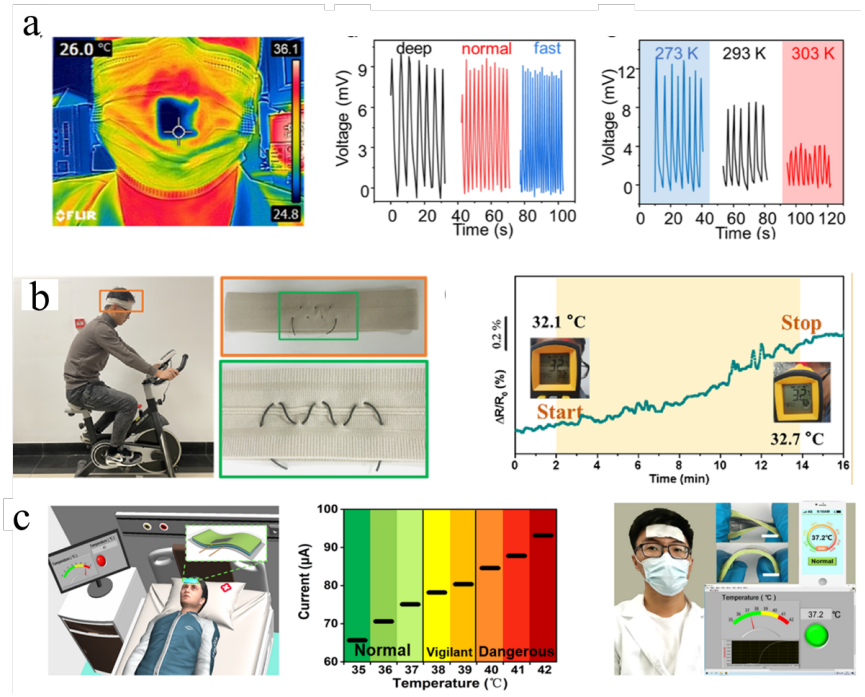

Figure 10 (a) Proof of Concept of Dual Network Thermoelectric Hydrogel Respiratory Monitoring System with Mask Attached, Infrared Image of Wearing Mask and Monitoring Results. Reprinted with permission from ref. 19. Copyright 2022 American Chemical Society. (b) The tester wore a headband with the sensor. The next is the response of the sensor when cycling. Reprinted with permission from ref. 89. Copyright 2022 American Chemical Society. (c) Panoramic view of the gel-based thermoelectric patch for body temperature monitoring. Relationship between current and body temperature in the three typical regions. Body temperature monitoring and the corresponding temperature signal are displayed on terminals. Insets: Photographs of the gel patch that was twisted and bent (scale bar: 1 cm). Reprinted with permission from ref. 20. Copyright 2021 American Chemical Society.

The thermoelectric gel patch prepared by Zhang et al.,[19] as illustrated in Figure 10a, effectively converted physiological data into easy-to-understand electrical pulse signals by taking advantage of the temperature difference between the environment and the heat generated by human breathing. Interestingly, the gel patch functioned reliably even in temperatures below 0 °C, implying its adaptability to low-temperature environments. In another investigation, Zhang et al. developed a highly-sensitive temperature sensor using thermoplastic polyurethane fiber that can accurately monitor human activity. The sensor, with a remarkable tensile strain of up to 270%, can be conveniently worn as a headband to monitor the body temperature of athletes (Figure 10b).[89] Similarly, Yang et al. successfully created a wearable temperature sensor using the oxidation-reduction reaction mechanism of $[Fe^{3+}/Fe^{2+}]$. The device generated variable current signals in response to fluctuations in body temperature, providing key information about the temperature status of the wearer, as shown in Figure 10c. These research findings may have significant relevance in monitoring human activity and predicting potential health risks, making them valuable contributions to the field.[20]In the latest progress, Zhang et al. introduced a thermogalvanic interpenetrating network hydrogel with $[Fe(CN)_6]^{3-}/[Fe(CN)_6]^{4-}$as a redox pair and KCl as a ion provider for thermodiffusion, which not only has good flexibility but also prominent thermoelectric property with the thermal current up to 124 μA at the temperature difference of 10 K. Committed to providing more effective medical assistance services.[102]

2.3.2. Integrated applications

The energy output of a single small thermoelectric hydrogel is relatively small and may be insufficient to meet real-life needs. To address this issue, integrated modules came into view. Most of the integrated modules are typically island-bridge structures with hundreds of small hydrogels connected in series and encapsulated together. Once the integrated module is successfully prepared, it not only enhances the energy output but also improves the overall application of thermoelectric hydrogel. The mechanical properties of the hydrogel can vary depending on the choice of matrix and crosslinking agents used in its preparation. The use of an integrated module unleashes the flexibility, strength, ductility, and toughness of the thermoelectric hydrogel.

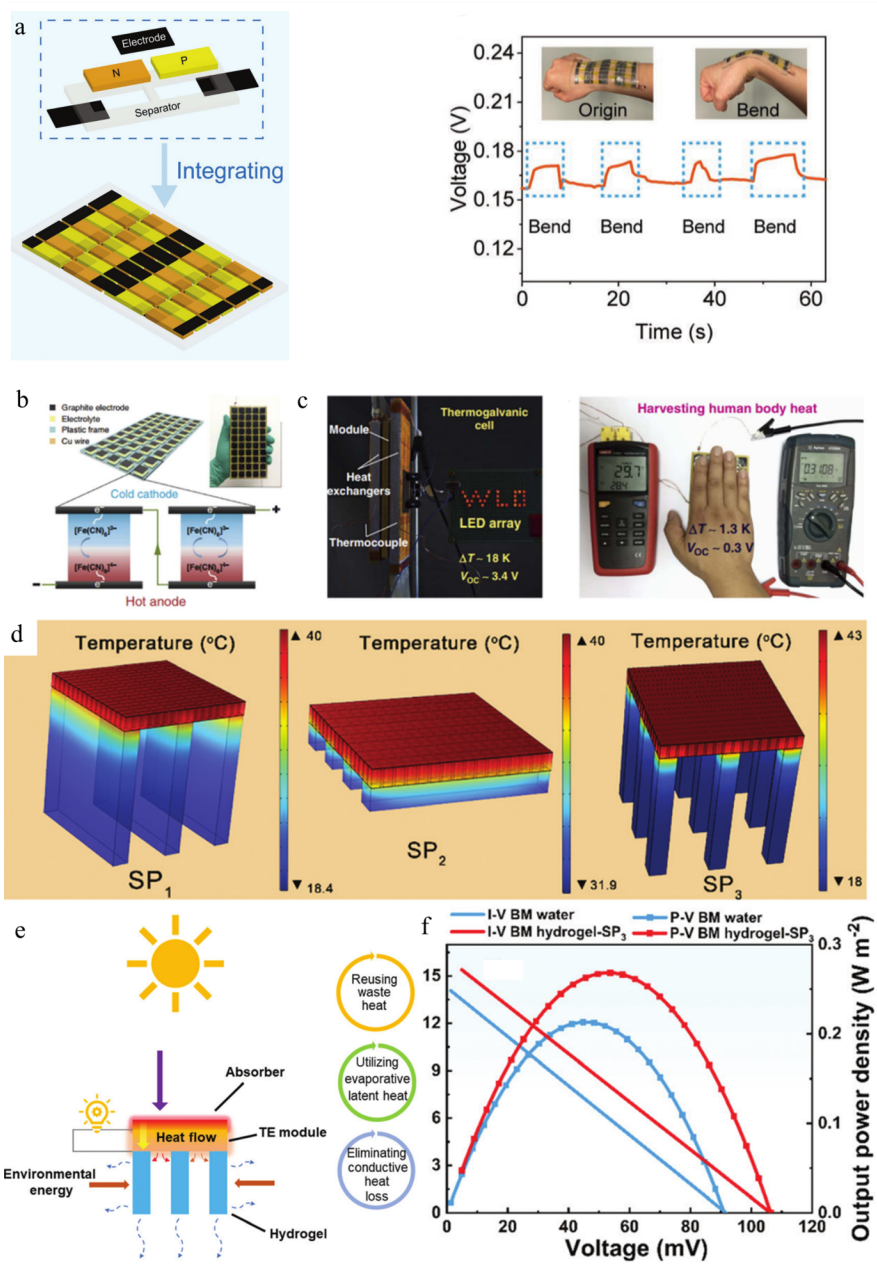

Figure 11 (a) Retractable schematic diagram of integrated wearable thermoelectric hydrogel batteries for energy collection. The thermoelectric properties of integrated 14 p-n couples of thermoelectric cells were

studied, and the voltage changes of the equipment attached to the deformed wrist were studied.[75] Reproduced from ref. 75 with permission from John Wiley and Sons, copyright 2022. (b) Integrated module representation diagram and schematic diagram. (c) The left diagram shows the power supply to the LEDs relying on the different temperatures of the contact water. The right diagram shows the voltage output of the integrated module collecting human waste heat. Reproduced with permission from ref. 75. Copyright 2018, Nature Publishing Group. (d) The temperature simulations of three types cogenerators. (e) The diagram of the proposed hybrid cogenerator for electricity and water. (f) The curves of current–voltage (I–V) and output power density–voltage (P–V) of different hybrid cogenerators under 1 kW m^{-2} illumination. Reproduced with permission from ref. 91. Copyright 2022, Royal Society of Chemistry.

Figure 11a[75] depicts a p-n battery integration module using$Fe(ClO_4)_2/Fe(ClO_4)_3$ as the n-type ion couple and $K_3[Fe(CN)_6]/K_4[Fe\ (CN)_6]$ as the p-type ion couple. The p-n to hydrogel electrolyte exhibited a voltage output of 29 mV, a current output of 8.5 Am^{-2}, and an average maximum power density of 0.66 mW K^{-2} m^{-2} per p-n cell at ΔT of 10 K. By integrating the hydrogel electrolyte with graphite paper electrodes, a close-fitting portable thermal battery device was fabricated, achieving a voltage output of 0.16 V with 14 couples of p-n batteries ($\Delta T = 4.1$ K). Figure 11b[8]illustrates the replacement of 50 thermoelectric hydrogels with integrated modules, as demonstrated by Xu et al. In this configuration, the hydrogels were utilized as batteries and interconnected in series using Cu wires. Figure 11c shows an aqueous electrolyte consisting of a mixture of urea (24 M), GdmCl (2.6 M), and 0.4 M of $K_3[Fe(CN)_6]/K_4[Fe(CN)_6]$. It was observed that the integrated module, when used with graphite as an electrode, exhibited an output voltage of 3.4 V and an output current of 1.2 mA at $\Delta T = 18$ K, which was sufficient to power the LEDs. Furthermore, Zhou et al.[90] used PVA as the matrix to prepare n-type and p-type thermoelectric hydrogels with $[Fe^{3+}/Fe^{2+}]$ and $[Fe(CN)_6]^{4-}/[Fe(CN)_6]^{3-}$as the respective redox couple. They connected, integrated, packaged, and attached 59 pairs of p-n hydrogels onto the human arm. At an ambient temperature of 5 °C, an output voltage of about 0.7 V and an output current of 2 μA was generated, with a corresponding maximum output power of 0.3 μW. Additionally, the integration of thermoelectric hydrogels has shown promising applications in the field of solar energy conversion. For this purpose, Miao et al. successfully developed a double-network hydrogel by combining AM with starch for the utilization of solar radiation to create a temperature gradient between the hot side of TEG and water, resulting in water evaporation and electricity generation (Figures 11d and 11e). The proposed design yields a high power density of up to 11.39 W m^{-2} and achieves multi-level utilization of solar energy (Figure 11f).[91] In recent research, Ma et al. once again prepared an excellent toughness thermogalvanic hydrogel thermocell for human health monitoring, with a high tensile strength of 19MPa and a high thermal power of 6.5mV K^{-1}.[100]

2.3.3. Heat collection and management devices

In addition, thermoelectric materials are used as a heat source for different applications to create a temperature difference between the hot and the cold ends. In this regard, Ma et al.[92] combined AM with sodium alginate to form double-network hydrogels and added guanidinium hydrochloride to enhance their thermoelectric properties and improve their heat dissipation ability. In this study, a 30 mm computer CPU was selected as the subject, and its normal operating temperature was observed to reach 76.2 °C. Notably, after applying the hydrogel onto the surface of the CPU, its operating temperature decreased by 15.1 °C, reaching 61.1 °C, while maintaining a stable voltage output of approximately 43.5 mV. At the same time, Ma and his team reported a multifunctional superelastic graphene-based thermoelectric sponge that is also committed to thermal management. It is not only relatively stable in performance, but also can cool the working CPU by 8K.[101] In another approach, Hu and co-workers[32] employed $K_3[Fe(CN)_6]/K_4[Fe(CN)_6]$ as redox couples in the electrolyte of thermochemical batteries and achieved evaporation and absorption of moisture through mutual regulation of Li^+ and Br^- ions. The researchers inserted a Ti plate in the middle of the hydrogel and placed two Ti meshes, one connected to a mobile phone cell as the positive pole and the other as the negative pole of the thermochemical batteries. This configuration resulted in varying temperatures during battery operation with different discharge efficiencies. Moreover, the studies illustrate that thermoelectric materials have promising prospects in the heat management of electronic devices.

3. Conclusions and Perspectives

Given the current global energy crisis, developing thermoelectric technologies is undoubtedly a good choice. However, traditional solid-state materials are no longer suitable for certain applications, leading to the emergence of quasi-solid-state gels as a promising alternative. In recent years, the research progress of thermoelectric hydrogels has advanced rapidly, especially in the development of quasi-solid-state thermoelectric hydrogels. According to the current research status, these materials have the potential for a diverse range of applications. This review provides an overview of the working principles and commonly used redox couples of thermocells based on the thermogalvanic effect. It then focuses on recent advances in hydrogel network matrices, electrode materials, surface and compositional structure of these thermocells. Lastly, the review presents the more advanced results in this field.

Despite significant progress in present thermoelectric research, there remains considerable scope for the development of thermoelectric batteries.

Firstly, the optimization of electrolytes is worth discussing. When hydrogels are used as electrolytes, the selection of different matrices and catalysts allows for the tailoring of their mechanical properties, with their ionic conductivity, thermal conductivity, and S. Currently, the $[Fe(CN)_6]^{4-}/[Fe(CN)_6]^{3-}$redox ion couple is the most intensively studied in terms of its thermoelectric effect. However, further exploration is needed to identify couples that exhibit a more prominent thermogalvanic effect. Additionally, we observed that the addition of reagents, such as NaCl and KCl, can enhance the efficiency of the oxidation-reduction process, thereby improving the overall$S$. Furthermore, the hydrogels achieved good working efficiency at both low and high temperatures by adding alcohol reagents. These three options provide opportunities for further optimization of the quasi-solid-state hydrogel electrolyte.

Besides, while addressing energy problems, the design of thermoelectric devices should not be confined to the laboratory setting but should also prioritize practicality in their structural design. The paper folding structure, pleated structures, helical structures, integrated textile structures, and island bridge structures with stretchable electrodes presented in this review offer various possible applications. Depending on the specific practical needs and material properties, different structures can be chosen to address problems in multiple environments, thus, making energy conversion more efficient.

Moreover, electrode materials play a critical role in the composition of batteries and should not be overlooked. Presently, metal electrodes are most commonly used, followed by carbon-based material electrodes, while thin film electrodes are rarely employed in battery applications. From the viewpoint of thermoelectric development, it is important to investigate the impact of the physical properties of electrodes on the overall performance. This call for a particular focus on flexible electrode materials with good mechanical properties, toughness, and low cost.

In conclusion, when studying thermogalvanic or thermal diffusion effects, the following steps involve optimizing the S, improving electrical conductivity, and reducing thermal conductivity. This can be achieved through effective cooperation among the electrolyte, structure design, and electrodes, along with the addition of suitable solvents. The rapid development of thermoelectric materials has demonstrated their enormous commercial potential, which can drive environmental and economic developments in the future.

Acknowledgement

This work was supported by the National Nature Science Foundation of China (51977079), Beijing Natural Science Foundation(3232054), the Key Laboratory of Icing and Anti/De-icing of CARDC (Grant No. IADL 20210401), the Central Guidance on Local Science and Technology Development Fund of Hebei Province (226Z1204G), the Top Young Innovative Talents of Colleges and Universities of Higher Learning Institutions of Hebei (BJ2021095), Youth Elite Scientists Sponsorship Program by Chinese Society for Electrical Engineering (CSEE-YESS-2017002), and the Fundamental Research Funds for the Central Universities (2020MS115)

References

1. Han, Y.; Zhang, J.; Hu, R.; Xu, D. High-thermopower polarized electrolytes enabled by methylcellulose for low-grade heat harvesting.*Sci. Adv* . **2022** , *8* , eabl5318.
2. Mu, K.; Mu, Y.; Wang, X.; Wu, X.; Pang, C.; Huang, Y.-T.; Feng, S.-P. Direct Thermal Charging Cell Using Nickel Hexacyanoferrate (II) Anode for Green Recycling of Low-Grade Heat. *ACS Energy Lett.***2022** , *7* , 1146-1153.
3. Li, T., Zhang, X.; Lacey, S.D; *et al.* Cellulose ionic conductors with high differential thermal voltage for low-grade heat harvesting. *Nat. Mater.* **2019,** *18* , 608–613.
4. Duan, J.; Yu, B.; Huang, L.; Hu, B.; Xu, M.; Feng, G.; Zhou, J. Liquid-state thermocells: Opportunities and challenges for low-grade heat harvesting. *Joule* **2021** , *5* , 768-779.
5. Yu, B.; Duan, J.; Cong, H.; Xie, W.; Liu, R.; Zhuang, X.; Wang, H.; Qi, B.; Xu, M.; Wang, Z. L.; Zhou, J. Thermosensitive crystallization-boosted liquid thermocells for low-grade heat harvesting. *Science* **2020** , *370* , 342-346.
6. Li, W.; Ma, J.; Qiu, J.; Wang, S. Thermocells-enabled low-grade heat harvesting: challenge, progress, and prospects. *Materials Today Energy* **2022** , *27* , 101032.
7. Zhao, W.; Wang, Z.; Hu, R.; Luo, X. Gel-based thermocells for low-grade heat harvesting. *EPL (Europhysics Letters)***2021** , *135,* 26001.
8. Duan, J.; Feng, G.; Yu, B. *et al.* Aqueous thermogalvanic cells with a high Seebeck coefficient for low-grade heat harvest. *Nat. Commun.* **2018** , *9* , 5146.
9. Zong, Y.; Li, H.; Li, X.; Lou, J.; Ding, Q.; Liu, Z.; Jiang, Y.; Han, W. Bacterial cellulose-based hydrogel thermocells for low-grade heat harvesting. *Chem. Eng. J.* **2022** , *433* , 134550.
10. Xie, G.; Li, P.; Zhang, Z.; Xiao, K.; Kong, X.-Y.; Wen, L.; Jiang, L. Skin-Inspired Low-Grade Heat Energy Harvesting Using Directed Ionic Flow through Conical Nanochannels. *Adv. Energy Mater.***2018** , *8* , 1800459.
11. Wei, X.; Zhao, Z.; Wang, L.; Jin, X.; Yuan, Z.; Wu, Z.; Wang, Z. L. Energy conversion system based on Curie effect and triboelectric nanogenerator for low-grade heat energy harvesting. *Nano Energy***2022** , *91* , 106652.
12. Li, Z.; An, Y.; Dong, S.; Chen, C.; Wu, L.; Sun, Y.; Zhang, X. Progress on zinc ion hybrid supercapacitors: Insights and challenges.*Energy Storage Mater.* **2020** , *31* , 252-266.
13. Li, Z.; Xu, Y.; Wu, L. *et al.* Zinc ion thermal charging cell for low-grade heat conversion and energy storage. *Nat. Commun.* **2022** , *13* , 132.
14. Hu, L.; Wu, H.; Zhu, T.; Fu, C.; He, J.; Ying, P.; Zhao, X. Tuning Multiscale Microstructures to Enhance Thermoelectric Performance of n-Type Bismuth-Telluride-Based Solid Solutions. *Adv. Energy Mater.* **2015** , *5* , 1500411.
15. Bai, C.; Li, X.; Cui, X.; Yang, X.; Zhang, X.; Yang, K.; Wang, T.; Zhang, H. Transparent stretchable thermogalvanic PVA/gelation hydrogel electrolyte for harnessing solar energy enabled by a binary solvent strategy. *Nano Energy* **2022** , *100* , 107449.
16. Cheng, H.; He, X.; Fan, Z.; Ouyang, J. Flexible Quasi-Solid State Ionogels with Remarkable Seebeck Coefficient and High Thermoelectric Properties. *Adv. Energy Mater.* **2019** , *9* , 1901085.
17. Horike, S.; Wei, Q.; Kirihara, K.; Mukaida, M.; Sasaki, T.; Koshiba, Y.; Fukushima, T.; Ishida, K. Outstanding Electrode-Dependent Seebeck Coefficients in Ionic Hydrogels for Thermally Chargeable Supercapacitor near Room Temperature. *ACS Appl Mater Interfaces***2020** , *12* , 43674-43683.
18. Lei, Z.; Gao, W.; Wu, P. Double-network thermocells with extraordinary toughness and boosted power density for continuous heat harvesting.*Joule* **2021** , *5* , 2211-2222.
19. Li, X.; Li, J.; Wang, T.; Khan, S. A.; Yuan, Z.; Yin, Y.; Zhang, H. Self-Powered Respiratory Monitoring Strategy Based on Adaptive Dual-Network Thermogalvanic Hydrogels. *ACS Appl Mater Interfaces* **2022** , *14* , 48743-48751.
20. Bai, C.; Wang, Z.; Yang, S.; Cui, X.; Li, X.; Yin, Y.; Zhang, M.; Wang, T.; Sang, S.; Zhang, W.; Zhang, H. Wearable Electronics Based on the Gel Thermogalvanic Electrolyte for Self-Powered Human Health Monitoring. *ACS Appl Mater Interfaces* **2021** , *13* , 37316-37322.
21. Liu, C.; Li, Q.; Wang, S.; Liu, W.; Fang, N. X.; Feng, S.-P. Ion regulation in double-network hydrogel module with ultrahigh thermopower for low-grade heat harvesting. *Nano Energy***2022** , *92* , 106738.

22. Peng, P.; Zhou, J.; Liang, L.; Huang, X.; Lv, H.; Liu, Z.; Chen, G. Regulating Thermogalvanic Effect and Mechanical Robustness via Redox Ions for Flexible Quasi-Solid-State Thermocells. *Nanomicro Lett.* **2022** , *14* , 81.
23. Kang, S.; Snyder, G. Charge-transport model for conducting polymers. *Nature Mater.* **2017,** *16* , 252–257.
24. Liu, Z.; Chen, G. Advancing Flexible Thermoelectric Devices with Polymer Composites. *Adv. Mater. Technol.* **2020** ,*5* , 2000049.
25. He, Z.; Zhou, Z.; Yuan, W. Highly Adhesive, Stretchable, and Antifreezing Hydrogel with Excellent Mechanical Properties for Sensitive Motion Sensors and Temperature-/Humidity-Driven Actuators.*ACS Appl Mater Interfaces* **2022** , *14* , 38205-38215.
26. Yang, P.; Yang, J. L.; Liu, K.; Fan, H. J. Hydrogels Enable Future Smart Batteries. *ACS Nano* **2022** , *16* , 15528-15536.
27. Wang, P.; Zhang, X.; Duan, W.; Teng, W.; Liu, Y.; Xie, Q. Superhydrophobic Flexible Supercapacitors Formed by Integrating Hydrogel with Functional Carbon Nanomaterials. *Chin. J. Chem.***2021** , *39* , 1153-1158.
28. Rajasekharan Pillai, V.N.; Mutter, M. Synthetic hydrophilic polymers. *Naturwissenschaften* **1981,** *68* , 558–566.
29. Sabbagh, F.; Muhamad, I.I. Physical and Chemical Characterisation of Acrylamide-Based Hydrogels, Aam, Aam/NaCMC and Aam/NaCMC/MgO. *J. Inorg. Organomet. Polym.* **2017** ,*27* , 1439–1449.
30. He, Y.; Wang, F.; Wang, X.; Zhang, J.; Wang, D.; Huang, X. A photocurable hybrid chitosan/acrylamide bioink for DLP based 3D bioprinting. *Mater. Des.* **2021** , *202,* 109588.
31. Peng, K.; Yang, K.; Fan, Y.; Yasin, A.; Hao, X.; Yang, H. Thermal/Light Dual-Activated Shape Memory Hydrogels Composed of an Agarose/Poly(acrylamide-co-acrylic acid) Interpenetrating Network.*Macromol. Chem. Phys.* **2017** , *218* , 1700170.
32. Pu, S.; Liao, Y.; Chen, K.; Fu, J.; Zhang, S.; Ge, L.; Conta, G.; Bouzarif, S.; Cheng, T.; Hu, X.; Liu, K.; Chen, J. Thermogalvanic Hydrogel for Synchronous Evaporative Cooling and Low-Grade Heat Energy Harvesting. *Nano Lett.* **2020** , *20* , 3791-3797.
33. Adelnia, H.; Ensandoost, R.; Shebbrin Moonshi, S.; Gavgani, J. N.; Vasafi, E. I.; Ta, H. T. Freeze/thawed polyvinyl alcohol hydrogels: Present, past and future. *Eur. Polym. J.* **2022** ,*164* , 110974.
34. Christie M. H.; Nikolaos A. P. Structure and Morphology of Freeze/Thawed PVA Hydrogels. *Macromolecules***2000,** *33* (7), 2472-2479.
35. He, Y.; Zhang, Q.; Cheng, H.; Liu, Y.; Shu, Y.; Geng, Y.; Zheng, Y.; Qin, B.; Zhou, Y.; Chen, S.; Li, J.; Li, M.; Odunmbaku, G. O.; Li, C.; Shumilova, T.; Ouyang, J.; Sun, K. Role of Ions in Hydrogels with an Ionic Seebeck Coefficient of 52.9 mV K(-1). *J. Phys. Chem. Lett.* **2022** , *13* , 4621-4627.
36. Lei, Z.; Gao, W.; Zhu, W.; Wu, P. Anti-Fatigue and Highly Conductive Thermocells for Continuous Electricity Generation. *Adv. Funct. Mater.* **2022** , *32* , 2201021.
37. Yang, S.; Tao, X.; Chen, W.; Mao, J.; Luo, H.; Lin, S.; Zhang, L.; Hao, J. Ionic Hydrogel for Efficient and Scalable Moisture-Electric Generation. *Adv. Mater.* **2022** , *34* , e2200693.
38. Yin, L.; Cao, M.; Kim, K. N.; Lin, M.; Moon, J.-M.; Sempionatto, J. R.; Yu, J.; Liu, R.; Wicker, C.; Trifonov, A.; Zhang, F.; Hu, H.; Moreto, J. R.; Go, J.; Xu, S.; Wang, J. A stretchable epidermal sweat sensing platform with an integrated printed battery and electrochromic display. *Nat. Electron.* **2022** , *5* , 694-705.
39. Chang, C.; Lue, A.; Zhang, L. Effects of Crosslinking Methods on Structure and Properties of Cellulose/PVA Hydrogels. *Macromol. Chem. Phys.* **2008** , *209* , 1266-1273.
40. Kumar, A.; Han, S. S. PVA-based hydrogels for tissue engineering: A review. *Int. J. Polym. Mater. Polym. Biomater.* **2016** ,*66* , 159-182.
41. Petty-Weeks, S.; Polak A.J. Differential scanning calorimetry and complex admittance analysis of PVA/H_3PO_4 proton conducting polymer blends. *Sens. Actuators* **1987** , *11(4),* 337-386.
42. Ngai, K.S.; Ramesh, S.; Ramesh, K. *et al.* A review of polymer electrolytes: fundamental, approaches and applications. *Ionics* **2016** , *22* , 1259–1279.

43. Zhang, J.; Yao, X.; Misra, R. K.; Cai, Q.; Zhao, Y. Progress in electrolytes for beyond-lithium-ion batteries. *J. Mater. Sci. Technol.* **2020** , *44* , 237-257.
44. Sharma, B.; Malik, P.; Jain, P. Biopolymer reinforced nanocomposites: A comprehensive review. *Mater. Today Commun.* **2018** ,*16* , 353-363.
45. Zou, D.; Nunes, S. P.; Vankelecom, I. F. J.; Figoli, A.; Lee, Y. M. Recent advances in polymer membranes employing non-toxic solvents and materials. *Green Chem.* **2021** , *23* , 9815-9843.
46. Fu, F.; Yang, D.; Zhang, W.; Wang, H.; Qiu, X. Green self-assembly synthesis of porous lignin-derived carbon quasi-nanosheets for high-performance supercapacitors. *Chem. Eng. J.* **2020** ,*392* , 123721.
47. Chen, B.; Chen, Q.; Xiao, S.; Feng, J.; Zhang, X.; Wang, T. Giant negative thermopower of ionic hydrogel by synergistic coordination and hydration interactions. *Sci. Adv.* **2021** , *7* , eabi7233.
48. Gao, W.; Lei, Z.; Zhang, C.; Liu, X.; Chen, Y. Stretchable and Freeze-Tolerant Organohydrogel Thermocells with Enhanced Thermoelectric Performance Continually Working at Subzero Temperatures. *A Adv. Funct. Mater.* **2021** ,*31* , 2104071.
49. Milowska, K. Z.; Majewski, J. A. Functionalization of carbon nanotubes with -CH(n), -NH(n) fragments, -COOH and -OH groups. *J. Chem. Phys.* **2013** , *138* , 194704.
50. Pal, K.; Banthia, A. K.; Majumdar, D. K. Preparation and characterization of polyvinyl alcohol-gelatin hydrogel membranes for biomedical applications. *AAPS PharmSciTech* **2007** ,*8* , 21.
51. Lee, H. Y.; Park, S. H.; Kim, J. H.; Kim, M. S. Temperature-responsive hydrogels via the electrostatic interaction of amphiphilic diblock copolymers with pendant-ion groups. *Polym. Chem.* **2017** ,*8* , 6606-6616.
52. Han, C.-G.; Qian, X.; Li, Q.; Deng, B.; Zhu, Y.; Han, Z.; Zhang, W.; Wang, W.; Feng, S.-P.; Chen, G.; Liu, W. Giant thermopower of ionic gelatin near room temperature. *Science* **2020** ,*368* , 1091-1098.
53. Lei, W.; Khan, S.; Chen, L.; Suzuki, N.; Terashima, C.; Liu, K.; Fujishima, A.; Liu, M. Hierarchical structures hydrogel evaporator and superhydrophilic water collect device for efficient solar steam evaporation. *Nano Res.* **2021** , *14* , 1135-1140.
54. Simič, R.; Yetkin, M.; Zhang, K.; Spencer, N. D. Importance of Hydration and Surface Structure for Friction of Acrylamide Hydrogels.*Tribol. Lett.* **2020** , *68* , 64.
55. Hua, J.; Ng, P. F.; Fei, B. High-strength hydrogels: Microstructure design, characterization and applications. *J. Polym. Sci., Part B: Polym. Phys.* **2018** , *56* , 1325-1335.
56. Mu, Q.; Cui, K.; Wang, Z. J.; Matsuda, T.; Cui, W.; Kato, H.; Namiki, S.; Yamazaki, T.; Frauenlob, M.; Nonoyama, T.; Tsuda, M.; Tanaka, S.; Nakajima, T.; Gong, J. P. Force-triggered rapid microstructure growth on hydrogel surface for on-demand functions. *Nat. Commun.***2022** , *13* , 6213.
57. Koh, W.-G.; Revzin, A.; Pishko, M. V. Poly(ethylene glycol) Hydrogel Microstructures Encapsulating Living Cells. *Langmuir***2002** , *18* , 2459-2462.
58. Sarker, B.; Papageorgiou, D. G.; Silva, R.; Zehnder, T.; Gul-E-Noor, F.; Bertmer, M.; Kaschta, J.; Chrissafis, K.; Detsch, R.; Boccaccini, A. R. Fabrication of alginate–gelatin crosslinked hydrogel microcapsules and evaluation of the microstructure and physico-chemical properties. *J. Mater. Chem. B* **2014** ,*2* , 1470-1482.
59. Revzin, A.; Russell, R. J.; Yadavalli, V. K.; Koh, W.-G.; Deister, C.; Hile, D. D.; Mellott, M. B.; Pishko, M. V. Fabrication of Poly(ethylene glycol) Hydrogel Microstructures Using Photolithography.*Langmuir* **2001** , *17* , 5440-5447.
60. Zhang, Y.; Chen, H.; Li, J. Recent advances on gelatin methacrylate hydrogels with controlled microstructures for tissue engineering.*IInt. J. Biol. Macromol.* **2022** , *221* , 91-107.
61. Yang, W.; Yu, H.; Liang, W.; Wang, Y.; Liu, L. Rapid Fabrication of Hydrogel Microstructures Using UV-Induced Projection Printing. *Micromachines* **2015** , *6* , 1903-1913.
62. Guan, J.; He, H.; Hansford, D. J.; Lee, L. J. Self-Folding of Three-Dimensional Hydrogel Microstructures. *J. PHYS. CHEM. B***2005** , *109* , 23134-23137.
63. Fukuie, K.; Iwata, Y.; Iwase, E. Design of Substrate Stretchability Using Origami-Like Folding Deformation for Flexible Thermoelectric Generator. *Micromachines* **2018** , *9* , 315.
64. Zou, J.; Wu, S.; Chen, J.; Lei, X.; Li, Q.; Yu, H.; Tang, S.; Ye, D. Highly Efficient and Environmentally Friendly Fabrication of Robust, Programmable, and Biocompatible Anisotropic, All-Cellulose, Wrinkle-

Patterned Hydrogels for Cell Alignment. *Adv. Mater.***2019** , *31* , e1904762.
65. Kato, M.; Kashihara, Y.; Asoh, T.-A.; Uyama, H. Geometry Control of Wrinkle Structures Aligned on Hydrogel Surfaces. *Langmuir***2020** , *36* , 1467-1473.
66. Kim, J. Y.; Oh, J. Y.; Lee, T. I. Multi-dimensional nanocomposites for stretchable thermoelectric applications. *Appl. Phys. Lett.***2019** , *114* , 043902.
67. Guan, Q.-F.; Han, Z.-M.; Zhu, Y.; Xu, W.-L.; Yang, H.-B.; Ling, Z.-C.; Yan, B.-B.; Yang, K.-P.; Yin, C.-H.; Wu, H.; Yu, S.-H. Bio-Inspired Lotus-Fiber-like Spiral Hydrogel Bacterial Cellulose Fibers. *Nano Lett.* **2021** , *21* , 952-958.
68. Nan, K.; Kang, S. D.; Li, K.; Yu, K. J.; Zhu, F.; Wang, J.; Dunn, A. C.; Zhou, C.; Xie, Z.; Agne, M. T.; Wang, H.; Luan, H.; Zhang, Y.; Huang, Y.; Snyder, G. J.; Rogers, J. A. Compliant and stretchable thermoelectric coils for energy harvesting in miniature flexible devices. *Sci. Adv.* , *4* , eaau5849.
69. Liu, J.; Zhu, Z.; Zhou, W.; Liu, P.; Liu, P.; Liu, G.; Xu, J.; Jiang, Q.; Jiang, F. Flexible metal-free hybrid hydrogel thermoelectric fibers. *J. Mater. Sci.* **2020** , *55* , 8376-8387.
70. Sun, T.; Zhou, B.; Zheng, Q.; Wang, L.; Jiang, W.; Snyder, G. J. Stretchable fabric generates electric power from woven thermoelectric fibers. *Nat. Commun.* **2020** , *11* , 572.
71. Hao, Y.; He, X.; Wang, L.; Qin, X.; Chen, G.; Yu, J. Stretchable Thermoelectrics: Strategies, Performances, and Applications. *Adv. Funct. Mater.* **2021** , *32* , 2109790.
72. Sun, T.; Wang, L.; Jiang, W. Pushing thermoelectric generators toward energy harvesting from the human body: Challenges and strategies. *Mater. Today* **2022** , *57* , 121-145.
73. Wang, C.; Wang, C.; Huang, Z.; Xu, S. Materials and Structures toward Soft Electronics. *Adv. Mater.* **2018** , *30* , e1801368.
74. Sun, T.; Wang, L.; Jiang, W.: Chapter 2 - Stretchable thermoelectric materials/devices for low-grade thermal energy harvesting. In *Low-Grade Thermal Energy Harvesting* ; Wang, S., Ed.; Woodhead Publishing, **2022** ; pp 11-40.
75. Xu, C.; Sun, Y.; Zhang, J.; Xu, W.; Tian, H. Adaptable and Wearable Thermocell Based on Stretchable Hydrogel for Body Heat Harvesting. *Adv. Energy Mater.* **2022** , *12* , 2201542.
76. Feng, L.; Wang, K.; Zhang, X.; Sun, X.; Li, C.; Ge, X.; Ma, Y. Flexible Solid-State Supercapacitors with Enhanced Performance from Hierarchically Graphene Nanocomposite Electrodes and Ionic Liquid Incorporated Gel Polymer Electrolyte. *Adv. Funct. Mater.***2018** , *28* , 1704463.
77. Lu, J.; Xiong, T.; Zhou, W.; Yang, L.; Tang, Z.; Chen, S. Metal Nickel Foam as an Efficient and Stable Electrode for Hydrogen Evolution Reaction in Acidic Electrolyte under Reasonable Overpotentials. *ACS ACS Appl. Mater. Interfaces* **2016** , *8* , 5065-5069.
78. Zhao, J.; Zheng, X.; Deng, Y.; Li, T.; Shao, Y.; Gruverman, A.; Shield, J.; Huang, J. Is Cu a stable electrode material in hybrid perovskite solar cells for a 30-year lifetime? *Energy Environ. Sci.* **2016** , *9* , 3650-3656.
79. Cattin, L.; El Mahlali, A.; Cherif, M. A.; Touihri, S.; El Jouad, Z.; Mouchaal, Y.; Blanchard, P.; Louarn, G.; Essaidi, H.; Addou, M.; Khelil, A.; Torchio, P.; Bernède, J. C. New dielectric/metal/dielectric electrode for organic photovoltaic cells using Cu:Al alloy as metal. *J. Alloys Compd.* **2020** ,*819* , 152974.
80. Bi, Y. G.; Liu, Y. F.; Zhang, X. L.; Yin, D.; Wang, W. Q.; Feng, J.; Sun, H. B. Ultrathin Metal Films as the Transparent Electrode in ITO-Free Organic Optoelectronic Devices. *Adv. Opt. Mater.***2019** , *7* , 1800778.
81. Jung, S.-M.; Kwon, J.; Lee, J.; Han, I. K.; Kim, K.-S.; Kim, Y. S.; Kim, Y.-T. Cost-efficient nickel-based thermo-electrochemical cells for utilizing low-grade thermal energy. *J. Power Sources***2021** , *494* , 229705.
82. Yu, B.; Xiao, H.; Zeng, Y.; Liu, S.; Wu, D.; Liu, P.; Guo, J.; Xie, W.; Duan, J.; Zhou, J. Cost-effective n-type thermocells enabled by thermosensitive crystallizations and 3D multi-structured electrodes. *Nano Energy* **2022** , *93* , 106795.
83. Jung, S.-M.; Kwon, J.; Lee, J.; Lee, B.-J.; Kim, K.-S.; Yu, D.-S.; Kim, Y.-T. Hybrid thermo-electrochemical energy harvesters for conversion of low-grade thermal energy into electricity via tungsten electrodes. *Appl. Energy* **2021** , *299* , 117334.

84. Berggren, M.; Malliaras, G. G. How conducting polymer electrodes operate. *Science* **2019** , *364* , 233-234.
85. Horike, S.; Wei, Q.; Kirihara, K.; Mukaida, M.; Koshiba, Y.; Ishida, K. Anomalous n-type conversion of thermoelectric polarity in ionic hydrogels using PEDOT:PSS electrodes. *J. Mater. Chem. C***2021** , *9* , 15813-15819.
86. Jia, Z.; Wang, Z.; Xu, C.; Liang, J.; Wei, B.; Wu, D.; Zhu, S. Study on poly(methyl methacrylate)/carbon nanotube composites. *Mat. Sci. Eng. A* **1999** , *271* , 395-400.
87. Kim, K. T.; Choi, S. Y.; Shin, E. H.; Moon, K. S.; Koo, H. Y.; Lee, G.-G.; Ha, G. H. The influence of CNTs on the thermoelectric properties of a CNT/Bi2Te3 composite. *Carbon* **2013** ,*52* , 541-549.
88. He, Y.; Lin, X.; Feng, Y.; Luo, B.; Liu, M. Carbon Nanotube Ink Dispersed by Chitin Nanocrystals for Thermoelectric Converter for Self-Powering Multifunctional Wearable Electronics. *Adv. Sci.***2022** , *9* , 2204675.
89. Li, F.; Xue, H.; Lin, X.; Zhao, H.; Zhang, T. Wearable Temperature Sensor with High Resolution for Skin Temperature Monitoring. *ACS Appl. Mater. Interfaces* **2022** , *14* , 43844-43852.
90. Yang, P.; Liu, K.; Chen, Q.; Mo, X.; Zhou, Y.; Li, S.; Feng, G.; Zhou, J. Wearable Thermocells Based on Gel Electrolytes for the Utilization of Body Heat. *Angew Chem. Int. Ed. Engl.* **2016** ,*55* , 12050-12053.
91. Mu, X.; Zhou, J.; Wang, P.; Chen, H.; Yang, T.; Chen, S.; Miao, L.; Mori, T. A robust starch–polyacrylamide hydrogel with scavenging energy harvesting capacity for efficient solar thermoelectricity–freshwater cogeneration. *Energy Environ. Sci.* **2022** , *15* , 3388-3399.
92. Zhang, D.; Mao, Y.; Ye, F.; Li, Q.; Bai, P.; He, W.; Ma, R. Stretchable thermogalvanic hydrogel thermocell with record-high specific output power density enabled by ion-induced crystallization. E*nergy Environ. Sci.* **2022** , *15* , 2974-2982.
93. Tian, C.; Bai, C.; Wang, T.; Yan, Z.; Zhang, Z.; Zhuo, K.; Zhang, H. Thermogalvanic hydrogel electrolyte for harvesting biothermal energy enabled by a novel redox couple of SO4/32- ions. *Nano Energy***2023** , *106.*
94. Fang, R.; Li, X.; Khan, S. A.; Wang, Z.; Cui, X.; Zhang, H.; Lin, Z.-H. Anhydrous Thermogalvanic Gel for Simultaneous Waste Heat Recovery and Thermal Management of Electronics. *ACS Appl. Polym. Mater.* **2023.**
95. Kim, T.; Lee, J. S.; Lee, G.; Yoon, H.; Yoon, J.; Kang, T. J.; Kim, Y. H. High thermopower of ferri/ferrocyanide redox couple in organic-water solutions. *Nano Energy* **2017** , *31* , 160-167.
96. Wang, H.; Zhuang, X.; Xie, W.; Jin, H.; Liu, R.; Yu, B.; Duan, J.; Huang, L.; Zhou, J. Thermosensitive-CsI3-crystal-driven high-power I-/I3- thermocells. *Cell Rep. Phys. Sci.* **2022** ,*3* , 100737.
97. Yin, P.; Geng, Y.; Zhao, L.; Meng, Q.; Xin, Z.; Luo, L.; Wang, B.; Mao, Z.; Sui, X.; Wu, W.; Feng, X. Robust and flexible bacterial cellulose-based thermogalvanic cells for low-grade heat harvesting in extreme environments. *Chem. Eng. J.* **2023** , *457.*
98. Wang, P.; Chen, T.; Zhang, X.; Duan, W.; Zhang, C.; Han, H.; Xie, Q. A Superhydrophobic Hydrogel for Self-Healing and Robust Strain Sensor with Liquid Impalement Resistance. *Chin. J. Chem.***2021** , *39* , 3393-3398.
99. Massetti, M.; Jiao, F.; Ferguson, A. J.; Zhao, D.; Wijeratne, K.; Wurger, A.; Blackburn, J. L.; Crispin, X.; Fabiano, S. Unconventional Thermoelectric Materials for Energy Harvesting and Sensing Applications. *Chem. Rev.* **2021** , *121* , 12465-12547.
100. Liu, L.; Zhang, D.; Bai, P.; Mao, Y.; Li, Q.; Guo, J.; Fang, Y.; Ma, R. Strong Tough Thermogalvanic Hydrogel Thermocell With Extraordinarily High Thermoelectric Performance. *Adv. Mater.***2023** , *n/a* , 2300696.
101. Zhang, D.; Mao, Y.; Bai, P.; Li, Q.; He, W.; Cui, H.; Ye, F.; Li, C.; Ma, R.; Chen, Y. Multifunctional Superelastic Graphene-Based Thermoelectric Sponges for Wearable and Thermal Management Devices.*Nano Lett.* **2022** , *22* , 3417-3424.]
102. Li, J.; Wang, Z.; Khan, S. A.; Li, N.; Huang, Z.; Zhang, H. Self-powered information conversion based on thermogalvanic hydrogel with interpenetrating networks for nursing aphasic patients.*Nano Energy* **2023** , *113* , 108612.

f

Manuscript received: XXXX, 2023 Manuscript revised: XXXX, 2023 Manuscript accepted: XXXX, 2023 Accepted manuscr